

# Oscillatory Electroosmotic Flow of Power-Law Fluids in a Microchannel

Rubén Baños, José Arcos, Oscar Bautista, Federico Méndez

**Abstract**—The Oscillatory electroosmotic flow (OEOF) in power law fluids through a microchannel is studied numerically. A time-dependent external electric field (AC) is suddenly imposed at the ends of the microchannel which induces the fluid motion. The continuity and momentum equations in the  $x$  and  $y$  direction for the flow field were simplified in the limit of the lubrication approximation theory (LAT), and then solved using a numerical scheme. The solution of the electric potential is based on the Debye-Hückel approximation which suggest that the surface potential is small, say, smaller than 0.025V and for a symmetric ( $z : z$ ) electrolyte. Our results suggest that the velocity profiles across the channel-width are controlled by the following dimensionless parameters: the angular Reynolds number,  $Re_\omega$ , the electrokinetic parameter,  $\bar{\kappa}$ , defined as the ratio of the characteristic length scale to the Debye length, the parameter  $\lambda$  which represents the ratio of the Helmholtz-Smoluchowski velocity to the characteristic length scale and the flow behavior index,  $n$ . Also, the results reveal that the velocity profiles become more and more non-uniform across the channel-width as the  $Re_\omega$  and  $\bar{\kappa}$  are increased, so oscillatory OEOF can be really useful in micro-fluidic devices such as micro-mixers.

**Keywords**—Oscillatory electroosmotic flow, Non-Newtonian fluids, power-law model, low zeta potentials.

## I. INTRODUCTION

**M**ICRO-FLUIDIC components such as micro-channels, micro-mixers and micro-pumps are commonly implemented in the design of biochips, for example electroosmosis has been well established as a micropumping technique used in many of these devices. Extensive studies about electroosmotic flow in microcapillaries have been reported in the literature, most of them considering the Debye-Hückel approximation [6], [7], some others regarding the time-dependent external electric field in Newtonian fluids [6], [8]. The rheology of the fluids is very important due to the immense application of microfluidic to analyze biofluids, in which may not be treated as Newtonian fluids. In this context, the rheology in electroosmotic flow with constant electric field (DC) has been extensively studied [9], [11], [12]. Lately, there are few studies considering both the rheology of the fluid and a time-dependent electrical field. Each effect has been studied in a separately manner, that is why our study consider an oscillatory electrical field which causes an oscillatory electroosmotic flow in the microchannel and the power-law model [10] to obtain the

Rubén Baños is with the ESIME Azcapotzalco, Instituto Politécnico Nacional, Av. de las Granjas No. 682, Col. Santa Catarina, Azcapotzalco, Ciudad de México, 02250, Mexico (e-mail: rdbm94@hotmail.com).

José Arcos and Oscar Bautista are with the ESIME Azcapotzalco, Instituto Politécnico Nacional, Av. de las Granjas No. 682, Col. Santa Catarina, Azcapotzalco, Ciudad de México, 02250, Mexico.

Federico Méndez is with the Universidad Nacional Autónoma de México, Coyoacan, Ciudad de México 04510, México.

velocity profiles across the microchannel-width as a function of the principal dimensionless parameters involved in the present investigation.

## II. PROBLEM FORMULATION

In Fig. 1 the schematic representation of the OEOF is shown. Consider a two-dimensional microchannel of height  $2h$  and length  $L$ , where  $L \gg h$ . The microchannel is filled with a symmetric electrolyte ( $z : z$ ) solution whose rheological behaviour follows the well-known Ostwald de Waele model. The anode and cathode at the ends of the microchannel provide a time-dependent electrical field which generates a periodically oscillatory flow via the electroosmotic effect.

### A. Electrical Field

The electrical potential in the location  $(x, y)$  in the microchannel, given by  $\Phi(x, y)$  arises by the superposition of the externally electric potential,  $\phi(x, y)$ , and the potential  $\psi(y)$  into the electrical double layer (with surface potential  $\zeta$ ). It is reasonable to assume that the electric potential is given by the linear superposition of the electrical double layer potential and the externally applied potential, which is valid for long microchannels [1]. Therefore, the Poisson-Boltzmann equation for a slit microchannel becomes,

$$\frac{d^2\psi}{dy^2} = -\frac{\rho_e}{\epsilon}. \quad (1)$$

From the above equation and the boundary conditions  $d\psi/dy = 0$  at  $y = 0$  and  $\psi = \zeta$  at  $y = h$ , the well-known solution for the distribution of the potential,  $\psi$ , with a free charge density defined as  $\rho_e = -\epsilon\kappa^2\psi$  is given by:

$$\bar{\psi} = \frac{\cosh \bar{\kappa}\bar{y}}{\cosh \bar{\kappa}} \quad (2)$$

where  $\bar{\psi} = \psi/\zeta$ ,  $\bar{\kappa} = \kappa h$  and  $\bar{y} = y/h$ .

### B. Velocity Field

To determine the flow field, we consider that  $\alpha = h/L \ll 1$ , therefore, the motion can be approximated as unidirectional [2]. The velocity components in the  $x$  and  $y$  directions are  $u = u(y, t)$  and  $v = 0$ , for  $t \geq 0$ . Also, neglecting external pressure gradient and gravity effects, the one-dimensional momentum equation is represented by,

$$\rho \frac{\partial u}{\partial t} = \frac{d\tau}{dy} + \rho_e E_x(t). \quad (3)$$

Equation (3) is subjected to the following boundary conditions. The symmetry boundary condition ( $du/dy=0$ ) was

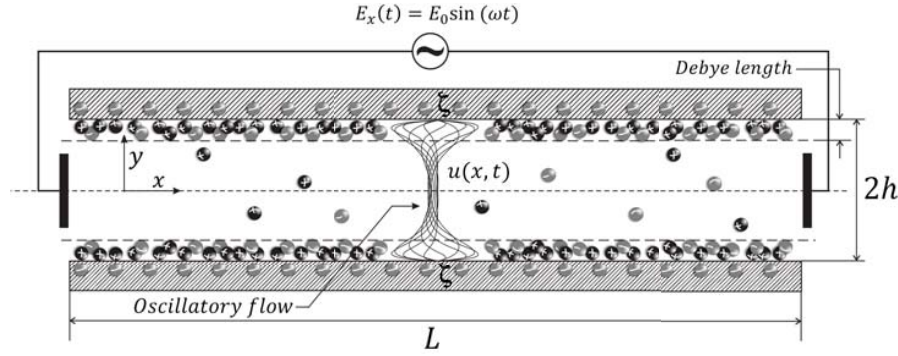


Fig. 1 Schematic model for an oscillatory electroosmotic flow moved by an externally electrical field defined by  $E_x(t) = E_0 \sin \omega t$ .  $E_0$  and  $\omega$  are the steady electric field and the angular frequency, respectively

established at the center of the microchannel, and both walls are subjected to the no-slip condition ( $u=0$ ), on the other hand due to the fluid starts from the rest an initial condition was required ( $u=0$  at  $t=0$ ). In (3), the externally electrical field is defined by  $E_x(t) = E_0 \sin \omega t$ .

The shear stress is defined as  $\tau = \mu (du/dy)$ , and the dynamic viscosity  $\mu$  for non-Newtonian fluids is related to the magnitude of shear rate via the power-law model [10],

$$\mu = m \left[ \left( \frac{du}{dy} \right)^2 \right]^{\frac{n-1}{2}}. \quad (4)$$

In (4) the parameters  $m$  and  $n$  are the consistency index and the behavior index of the flow. For values of  $n < 1$  and  $n > 1$  the shear-thinning and shear-thickening behavior are present, respectively; and for  $n = 1$  the Newtonian case was recovered. Using the definition of  $\rho_e$  given in Section II-A, (4) and the definition of the electrical field (3) rewritten as:

$$\rho \frac{\partial u}{\partial t} = \frac{\partial}{\partial y} \left\{ m \left[ \left( \frac{\partial u}{\partial y} \right)^2 \right]^{\frac{n-1}{2}} \frac{\partial u}{\partial y} \right\} - \epsilon \kappa^2 \zeta E_0 \frac{\cosh(\kappa y)}{\cosh(\kappa h)} \sin(\omega t) \quad (5)$$

Introducing the following dimensionless variables

$$\bar{u} = \frac{u}{U_{HS}} \quad \bar{v} = \frac{v}{(\alpha U_{HS})}$$

$$\bar{x} = \frac{x}{L} \quad \tau = \frac{\omega t}{2\pi}$$

where  $U_{HS} = -\epsilon \zeta E_0 / m$  is the Helmholtz-Smoluchowski velocity, the dimensionless momentum equation acquires the following form,

$$\frac{\rho_f \omega U_{HS}}{2\pi} \frac{\partial \bar{u}}{\partial \tau} = \frac{m U_{HS}}{h^2} \left( \frac{U_{HS}^2}{h^2} \right)^{\frac{n-1}{2}} \frac{\partial}{\partial \bar{y}} \left\{ \left[ \left( \frac{\partial \bar{u}}{\partial \bar{y}} \right)^2 \right]^{\frac{n-1}{2}} \frac{\partial \bar{u}}{\partial \bar{y}} \right\} - \bar{\kappa}^2 \frac{\cosh(\bar{\kappa} \bar{y})}{\cosh(\bar{\kappa})} \sin(2\pi \tau), \quad (6)$$

Manipulating algebraically is easy to show that

$$\frac{\partial}{\partial \bar{y}} \left\{ \left[ \left( \frac{\partial \bar{u}}{\partial \bar{y}} \right)^2 \right]^{\frac{n-1}{2}} \frac{\partial \bar{u}}{\partial \bar{y}} \right\} = n \left\{ \left[ \left( \frac{\partial \bar{u}}{\partial \bar{y}} \right)^2 \right]^{\frac{n-1}{2}} \frac{\partial^2 \bar{u}}{\partial \bar{y}^2} \right\}$$

From the above mentioned and rearranging (6), is obtained:

$$\frac{Re_\omega^2}{2\pi} \frac{\partial \bar{u}}{\partial \tau} = n (\lambda^2)^{\frac{n-1}{2}} \left\{ \left[ \left( \frac{\partial \bar{u}}{\partial \bar{y}} \right)^2 \right]^{\frac{n-1}{2}} \frac{\partial^2 \bar{u}}{\partial \bar{y}^2} \right\} + \bar{\kappa}^2 \frac{\cosh(\bar{\kappa} \bar{y})}{\cosh(\bar{\kappa})} \sin(2\pi \tau), \quad (7)$$

in (7),  $Re_\omega = h(\omega/\nu)^{1/2}$  is the angular Reynolds number, and the parameter  $\lambda = U_{HS}/h$ . With the follow dimensionless boundary and initial conditions:

$$\bar{u} = 0 \quad \text{at} \quad \bar{y} = 1$$

$$\frac{\partial \bar{u}}{\partial \bar{y}} = 0 \quad \text{at} \quad \bar{y} = 0$$

$$\bar{u} = 0 \quad \text{at} \quad \tau = 0$$

### III. SOLUTION METHODOLOGY

Equation (7) was solved numerically using the Crank-Nicolson method [3], [5], applying a central difference scheme in the following form [4],

$$-\theta_1 \bar{u}_{i+1}^{n+1} + \theta_2 \bar{u}_i^{n+1} - \theta_1 \bar{u}_{i-1}^{n+1} = \theta_3 \quad (8)$$

where,  $\theta_1$ ,  $\theta_2$  and  $\theta_3$  are defined as,

$$\theta_1 = \frac{A^g \gamma}{2\Delta \bar{y}^2} \quad (9)$$

$$\theta_2 = 2\theta_1 + \frac{1}{\Delta \tau} \quad (10)$$

$$\theta_3 = \frac{\bar{u}_i^n}{\Delta \tau} + \theta_1 (\bar{u}_{i+1}^n - 2\bar{u}_i^n + \bar{u}_{i-1}^n) + \eta. \quad (11)$$

In order to solve the non-linear equation (7)

$$A^g = \left[ \left( \frac{\partial \bar{u}}{\partial \bar{y}} \right)^2 \right]^{\frac{n-1}{2}} \quad (12)$$

is considered as a constant value leading to a second order differential equation.  $\Delta\tau$  and  $\Delta\bar{y}$  are the time step and the size step in the  $\bar{y}$  direction, respectively; and the parameters  $\gamma$  and  $\eta$  that appear in (8) and (11), are given as follows,

$$\gamma = \frac{2\pi n(\lambda^2)^{\frac{n-1}{2}}}{Re_\omega^2} \quad (13)$$

$$\eta = \frac{2\pi\bar{\kappa}^2 \cosh(\bar{\kappa}\bar{y})}{Re_\omega^2 \cosh(\bar{\kappa})} \sin(2\pi\tau) \quad (14)$$

The solution procedure starts providing initial guess values for  $A^g$ , a tridiagonal matrix algorithm is used to solve the system of equations. With the discrete values obtained,  $A^g$  was recalculated again and again until the required relative error of  $10^{-8}$  was achieved, this approximation is really useful because for values of  $\partial\bar{u}/\partial\bar{y} = 0$  and a behavior index  $n$  smaller than 1, the value of  $A^g$  is undetermined; so, in this way this value is very close to zero but never equal zero.

From (12) is clear that this value is varying in the  $\bar{y}$  direction so then it had to be recalculated for each node in the space and all this procedure was done for each node in the time.

#### IV. RESULTS AND DISCUSSION

In order to obtain numerical results, the values of the physical parameters that appear in (9)-(14), were considered as in follows:  $\rho \sim 10^3 \text{kg/m}^3$ ,  $m \sim 10^{-3} \text{Pa.s}^n$ ,  $\epsilon_0 \sim 10^{-10} \text{F/m}$ ,  $\epsilon_r \sim 10^2$ ,  $\zeta \ll 0.025 \text{V}$ , and  $E_0 \sim 10^3 \text{V/m}$ ,  $h = (100 - 5) \mu\text{m}$ . For the oscillation frequencies we consider values from 400Hz to 360kHz and Debye lengths from 15 to 300nm. Some of the estimated values used in the numerical calculations were,  $Re_\omega = 5, 15, 50$ , this the ratio of the viscous diffusion time-scale to the oscillation time-scale, the dimensionless Debye length  $\bar{\kappa} = 10, 50, 100$  and  $\lambda = 0.5, 1.5, 3$  which is the ratio of the Helmholtz-Smoluchowski velocity to the characteristic length scale.

Fig. 2 shows the velocity profile  $\bar{u}(\bar{y}, \tau)$  through the microchannel width, it can be seen how the velocity reverses its direction and is oscillating due the imposed electric field. This behavior is repeated in each period when a completely periodical flow is reached.

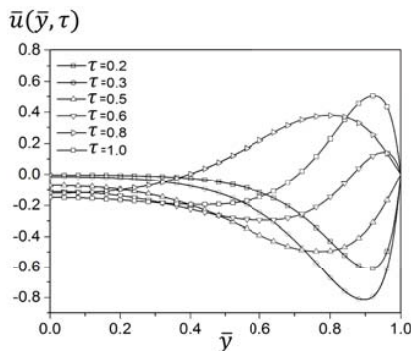


Fig. 2 Dimensionless velocity distribution  $\bar{u}(\bar{y}, \tau)$  vs  $\bar{y}$ , for various values of  $\tau$  at  $n = 0.8$ ,  $Re_\omega = 5$ ,  $\bar{\kappa} = 15$  and  $\lambda = 2$

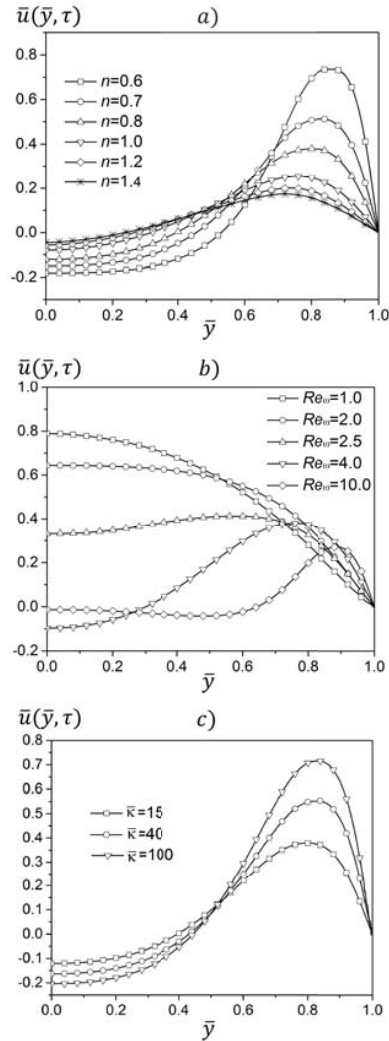


Fig. 3 Dimensionless velocity distribution  $\bar{u}(\bar{y}, \tau)$  vs  $\bar{y}$ , for various values of angular Reynolds number  $Re_\omega$ , dimensionless debye length  $\bar{\kappa}$  and the flow behavior index  $n$  at  $\lambda = 2$  and  $\tau = 1$ . (a)  $Re_\omega = 5$  and  $\bar{\kappa} = 15$ . (b)  $\bar{\kappa} = 15$  and  $n = 0.8$ . (c)  $n = 0.8$  and  $Re_\omega = 5$

Fig. 3 (a) shows the dimensionless velocity profile  $\bar{u}(\bar{y}, \tau)$  vs  $\bar{y}$  for various values of fluid behavior index at a fixed  $Re_\omega = 5$  and  $\bar{\kappa} = 15$ , it can be seen that the velocity magnitude is higher as  $n$  decreases, it is known that shear-tinning ( $n < 1$ ) have a lower viscosity than shear-thickening ( $n > 1$ ) fluids, so to less viscous fluids take a shorter time to attain a periodically behavior, the fluids motion begins near the surface of the microchannel, where the electroosmotic force is acting, there the profile has a parabolic shape with higher velocities and as it approaches to the center the velocity becomes negative close to zero.

Fig. 3 (b) shows  $\bar{u}(\bar{y}, \tau)$  for various values of  $Re_\omega$  at  $\bar{\kappa} = 15$  and  $n = 0.8$ , as the  $Re_\omega$  increases (higher frequencies of oscillation) the velocity profile is more non uniform and in opposite for smaller values it has a parabolic shape. Opposite to Fig. 2 (a), the velocity profile reach higher values near the center of the microchannel.

Fig. 3 (c) shows the effect of the electric double layer in the velocity, as  $\bar{\kappa}$  increases (which indicates shorter Debye lengths) the velocity becomes higher near to the wall of the microchannel and decrease as it approaches the center.

#### V. CONCLUSIONS

Oscillatory electroosmotic flow for non-Newtonian fluids was analyzed. The analysis revealed four main parameters that describe the dynamic behavior of the OEOF: the angular Reynolds number,  $Re_\omega$ , the electrokinetic parameter,  $\bar{\kappa}$ , defined as the ratio of the characteristic length scale to the Debye length, the parameter  $\lambda$  which represents the ratio of the Helmholtz-Smoluchowski velocity to the characteristic length scale and the flow behavior index,  $n$ . The principal conclusion are listed below:

- Using the Ostwald de Waele or Power-law model the results showed the different behaviors in the velocity distribution for shear-thinning and shear-thickening fluids, which is really important due to the extensive applications of microfluidic devices in biochemistry.
- For some processes in which is desired the mass transport it can be enhancement using lower frequencies of oscillation, which produce velocity profiles with a parabolic shape and this affects directly those processes.
- With proper choices of the Debye length and oscillation frequency the separation of species using oscillatory electroosmotic flow is achievable.

#### ACKNOWLEDGMENT

This work was granted by the Programa Institucional de Formación de Investigadores by 20180768 and 20180222 from SIP-IPN and the Fondo Sectorial de Investigación para la Educación from the Secretaria de Educación Pública-Consejo Nacional de Ciencia y Tecnología (No. CB-2013/220900). R. Baños acknowledges the support from CONACYT program for a MS in thermofluids grant at SEPI UA-ESIME of the Instituto Politécnico Nacional at Mexico.

#### REFERENCES

- [1] Masliyah, J. H., & Bhattacharjee, S. Electrokinetic and colloid transport phenomena. John Wiley & Sons.(2006)
- [2] Leal L. G. Advanced transport phenomena. Cambridge University Press. (2007)
- [3] Hoffman, J. D., & Frankel, S. Numerical methods for engineers and scientists. CRC press.(2001)
- [4] Pantakar, S. V. Numerical Heat Transfer and Fluid Flow. Hemisphere Publ., Washington.(1980)
- [5] Anderson, J. D., & Wendt, J. Computational fluid dynamics (Vol. 206). New York: McGraw-Hill.(1995)
- [6] Huang, H. F., & Lai, C. L. Enhancement of mass transport and separation of species by oscillatory electroosmotic flows. In Proceedings of the Royal Society of London A: Mathematical, Physical and Engineering Sciences (Vol. 462, No. 2071, pp. 2017-2038). The Royal Society.(2006)
- [7] Zhao, C., Zholkovskij, E., Masliyah, J. H., & Yang, C. Analysis of electroosmotic flow of power-law fluids in a slit microchannel. Journal of colloid and interface science, 326(2), 503-510.(2008)
- [8] Rojas, G., Arcos, J., Peralta, M., Méndez, F., & Bautista, O. Pulsatile electroosmotic flow in a microcapillary with the slip boundary condition. Colloids and Surfaces A: Physicochemical and Engineering Aspects, 513, 57-65.(2017)
- [9] Babaie, A., Sadeghi, A., & Saidi, M. H. Combined electroosmotically and pressure driven flow of power-law fluids in a slit microchannel. Journal of Non-Newtonian Fluid Mechanics, 166(14-15), 792-798.(2011)
- [10] Oswald, & A., Hernández-Ortiz J. P. Polymer Processing. Modeling and Simulation. Carl Hanser Verlag, Munich 2006
- [11] Zhao, C., & Yang, C. An exact solution for electroosmosis of non-Newtonian fluids in microchannels. Journal of Non-Newtonian Fluid Mechanics, 166(17-18), 1076-1079.(2011)
- [12] Qi, C., & Ng, C. O. Electroosmotic flow of a power-law fluid in a slit microchannel with gradually varying channel height and wall potential. European Journal of Mechanics-B/Fluids, 52, 160-168.(2015)